

Christopher Hartman, Jerry Y. Harrington*, and Johannes Verlinde
 Department of Meteorology, Pennsylvania State University, University Park, Pennsylvania

1. INTRODUCTION

The interaction between drop growth and radiative heating/cooling has been shown to have significant influences on the evolution of the drop size spectrum. This problem was first considered by Fuchs (1959) who concluded that infrared, or longwave (LW), radiative effects on drop growth are negligible in the interior of a cloud. However, Fuchs did not consider cloud boundaries where gradients in radiative fluxes are large, producing LW cooling and solar (SW) heating rates as large as -15 K hr^{-1} and 2 K hr^{-1} , respectively. Because of this, Roach (1976) and Barkstrom (1978) included LW radiative effects for individual drops and found that radiative cooling enhances condensation and allows larger drops ($r > 20 \mu\text{m}$) to grow even in a subsaturated environment.

Because radiative influences are size-dependent, Guzzi and Rizzi (1980) considered how a population of drops, growing by vapor diffusion only, are affected by LW cooling. They found that radiative cooling enhances larger, but suppresses smaller, drop growth. Fifteen years later, Austin et al. (1995) included collision-coalescence. Further, they derived an improved version of the equilibrium supersaturation ($s_{u,eq}$) equation including radiative effects. By using these improved formulations, Austin et al. found that collision-coalescence was enhanced by infrared radiative cooling, reducing the time required for the onset of precipitation by as much as a factor of four.

Beginning around 1990, one-dimensional (1D) models of stratocumulus clouds and fog were modified to include the radiative term. These microphysical-dynamical models showed that enhanced production of large drops due to radiation occurs within reasonable cloud time-scales. Bott et al. (1990) included the radiative term in their 1D fog model with bin microphysics and showed that observed oscillations of liquid water content (LWC) in fogs could only be reproduced if the radiative term were included. About five years later, Ackerman et al. (1995) used a 1D model coupled to bin microphysics with the radiative term to simulate marine stratocumulus. Their results showed a significant dependence of the LWC, optical depth, and supersaturation on the radiative term.

In order to examine LW radiative influences in a less parametrically constrained model, Harrington et al. (2000) included the radiative term in an eddy resolving model (ERM), the 2D counterpart of large eddy simulation (LES). Simula-

tions of arctic stratus were conducted with the ERM along with a trajectory ensemble model (TEM). This work showed that the radiative effect reduces the time required for the onset of drizzle by up to a half hour. Furthermore, Harrington et al.'s results showed that only long cloud-top trajectories, which are the parcels most likely to produce drizzle anyway, are significantly affected by radiative cooling. Finally, Harrington et al. also showed that the radius-dependence of the radiative term allows large drops to grow at the expense of small ($r < 10 \mu\text{m}$) drops.

In this paper, we extend the work of Harrington et al. by introducing strong solar heating to the problem

2. NUMERICAL MODEL AND CASE

The model used for these studies is the LES version of the Regional Atmospheric Modeling System (RAMS). The model includes liquid bin microphysics as modified by Stevens et al. (1996). Longwave and shortwave heating/cooling are computed with a two-stream radiative transfer model using 6 solar and 12 infrared bands. Optical properties for the bin model are computed using the method of Harrington and Olsson (2001) and included in the bin vapor growth equations following Harrington et al. (2000). Collision-coalescence, kinetic effects, curvature and solution terms are also included.

The stratocumulus case simulated is a variant of that described in Moeng et al. (1996). The LES model was run over 6 hours and for two cases: a case with LW cooling only (LES-LW), and a case with SW heating (LES-SW) for overhead sun. Each run was conducted for 6 hours.

During the simulation, 600 point parcels were released below cloud base at hour 4. These parcels were advected through the grid with thermodynamic, radiative, and dynamic information being written out every time-step for the remaining 2 hours of the simulation. These parcel time-series can then be used to force an off-line bin microphysical model (i.e. a TEM, see Feingold et al., 1996; Harrington et al., 2000). In other words, the microphysics follows the parcel and is forced by the vertical motion, thermodynamics, and radiation recorded by each parcel. The main idea here was to use a framework in which alterations in the microphysics could not feedback to the radiative cooling and dynamic motions of the stratus. It is this TEM that we use below in our examinations of the SW heating influences.

*Corresponding author address: J. Harrington, Dept. of Meteorology, Penn State University, University Park, PA, 16802.
 email: harring@mail.meteo.psu.edu

3. MODEL RESULTS

3.1 Cloud Time Scales

In-cloud time scales are one of the primary determinants of cloud microphysical characteristics. Hence, we have used our parcel data set to determine the average in-cloud residence time (τ_{incloud}) for each parcel in our data set. The histogram

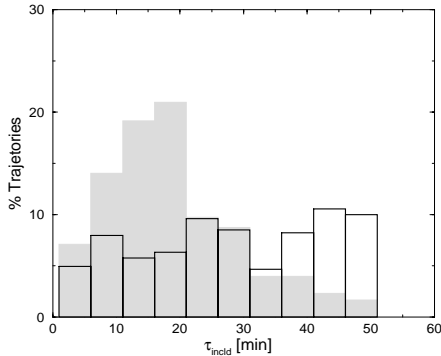


Figure 1. % of parcels with a given average in-cloud residence time for LW only (shaded) and LW+SW case (solid).

shown in Figure 1 illustrates this. For LES-LW, parcels cycle from cloud top (~ 850 m) through cloud base (~ 500 m) and to the surface. However, when SW radiation is included (overhead sun), cloud base is strongly stabilized and this confines most parcels to the cloud layer. Hence, the in-cloud residence time distribution is roughly flat (it is equally likely for a given trajectory to have a long time scale as to have a short time-scale.) This result may have important implications for collision coalescence which will discuss later.

Radiative influences have their strongest effects near cloud boundaries, hence cloud-top residence time of trajectories is important for quantifying our results. Cloud top in this case is defined as the region where LW cooling occurs. As one might expect, the distribution of cloud-top residence times for LES-SW is broader than for LES-LW (not shown). The average amount of time a trajectory spends at cloud top is 13 min in the LW case but is nearly 20 min in the SW case. Hence, on average, cloud-top radiative effects have almost 20 minutes to influence drop populations. In the analysis below, we consider only the LES-SW case.

3.2 Cloud-Top Trajectory Analysis

Given the above discussion, we first examine the effects of solar heating on one parcel from our 600 parcel trajectory set. This trajectory tracks along cloud top for an extended period of time, therefore providing a good example of radiation-altered drop growth. As Fig. 2 shows, this parcel entered an updraft below cloud base ($w_{\text{max}} \sim 0.5 \text{ m s}^{-1}$) around 270

min of simulation time and was advected to cloud top where it remained for 1 hour. LWC increases as the parcel rises and

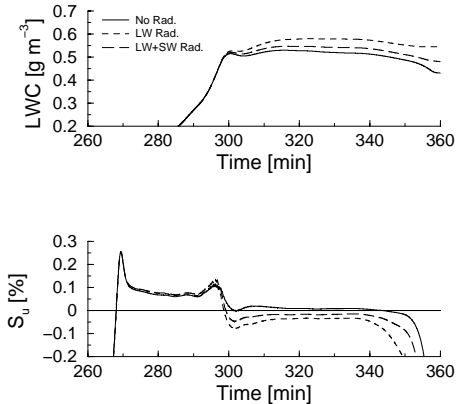


Figure 2. LWC and S_u for cases with and without the radiative term in the drop growth equation.

reaches a roughly constant value at cloud top. The supersaturation (S_u) shows a peak at cloud base (270 min) and a second, smaller peak near cloud top (vertical motions rose again near cloud top) before reaching a roughly constant value. When the radiative term is not included in the growth equation, the LWC is lower and S_u equilibrates near 0 (as expected). However, when only LW radiation is included in the growth equation, LWC increases at cloud top and S_u drops below zero. This latter effect was discussed in Harrington et al. (2000) and is due to the fact that $r > 10 \mu\text{m}$ drops can exist in a subsaturated environment. Logically, including SW heating reduces both of these effects.

Though this influence of SW heating on two macroscale cloud quantities is rather mundane, its differential effect on droplet growth is not. Figure 3 shows the mass size distribution

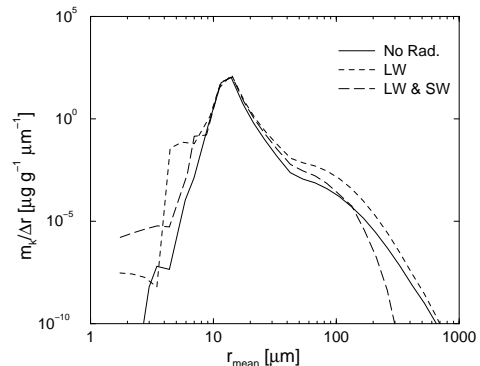


Figure 3. Mass size distribution after 15 min at cloud top for radiative and non-radiative influenced growth.

tion after 15 min of growth at cloud top. The case without radiative influences shows the standard cloud drop mode with a

larger drizzle mode beginning to appear. As in Harrington et al. (2000), the inclusion of LW effects enhances the collision-coalescence process leading to a broader size spectrum. Furthermore, a smaller drop mode begins to appear and is due to the fact that small drops ($r < 8$ to $10 \mu\text{m}$) are weakly influenced by the radiative effect and, therefore, evaporate in the slightly subsaturated environment.

Both of these general characteristics, though of lesser magnitude, are also evident in the case that includes SW heating. However, when SW heating is included, a significant

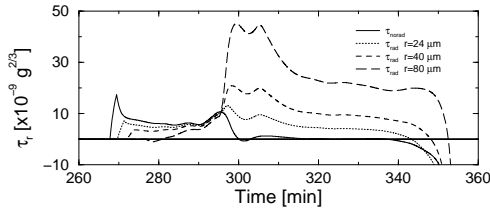


Figure 4. Supersaturation forcing for large drop bins including LW radiative effects only.

down-turn in the mass distribution occurs at $r > 150 \mu\text{m}$. In fact, the amount of mass at these sizes is lower than that of the case without the radiative term. Solar heating is causing a narrowing of the drop size spectrum preferentially at larger sizes. The reasons why this is the case can be understood by examining time-series plots of the supersaturation forcing (τ_r) for each drop bin. Figure 4 shows τ_r for the case without radiation

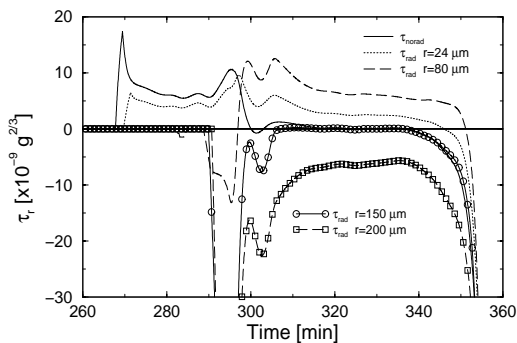


Figure 5. Supersaturation forcing for large drop bins with LW and SW radiative effects included.

(in this case, τ does not depend on size) and with LW radiative influences on drop growth. Since the radiative term in the drop growth equation increases with drop size, drops experience increasingly large growth rates the longer they spend exposed to LW cooling.

The inclusion of SW radiation has a strong effect on the vapor growth of large drops (Fig. 5). As expected, SW heating reduces the positive impact of LW cooling on drop growth (compare with Fig. 4). However, Fig. 5 shows that drops with $r \sim 150 \mu\text{m}$ experience almost zero growth rate while drops

larger than this size experience evaporation. For these large drops, SW heating is greater than LW cooling and, therefore, the larger drops experience a net warming. Since this net radiative warming increases with drop size, evaporation increases commensurately. This could place a damper on the further production of large drops, effectively reducing the strength of the collision-coalescence process. That SW absorption increases dramatically for larger drops has been known for sometime (e.g. Wiscombe et al., 1984). However, the supersaturation influence that we show here has not been examined before. See our companion paper (Harrington and Hartman, 2002) in this conference volume for an extended discussion of SW influences on supersaturation.

4. ENSEMBLE PARCEL RESULTS

Though intriguing, the above results are only for a single, cloud-top tracking parcel out of a set of 600 total trajectories. In this section, we illustrate the above discussed effects in the context of simulations that include all 600 parcels. Of particular interest, from a cloud-scale perspective, are the influences of SW heating on drop growth and the indirect influence this has on collision-coalescence.

4.1 Ensemble View of Growth Rates

A cloud-scale perspective of the importance of both LW cooling and SW heating on drop growth can be gained by examining the supersaturation forcing (τ_r). As was stated above, the supersaturation forcing is not dependent on size for drops $> 10 \mu\text{m}$ if radiative effects are not included. Figure 6

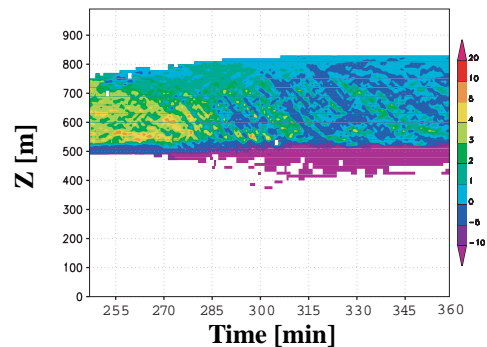


Figure 6. Supersaturation forcing (τ_r) for $15 \mu\text{m}$ cloud drops as a function of time and with no radiative term.

shows τ_r shaded for all 600 parcels as a function of height and time. Parcels moving within updrafts and downdrafts cross on this image since, at times, different parcels are moving within updrafts and downdrafts at the same height, but at different horizontal locations. Downdrafts (blue regions descending from cloud top) are subsaturated, hence drops are evaporating whereas updrafts, which are less easy to discern, show slight supersaturations. The region below cloud base shows that

strong evaporation is occurring (purple region) while cloud top has nearly zero supersaturation, and hence forcing.

The case is, of course, different if the radiative term is included in drop vapor growth. Drop growth rates of very

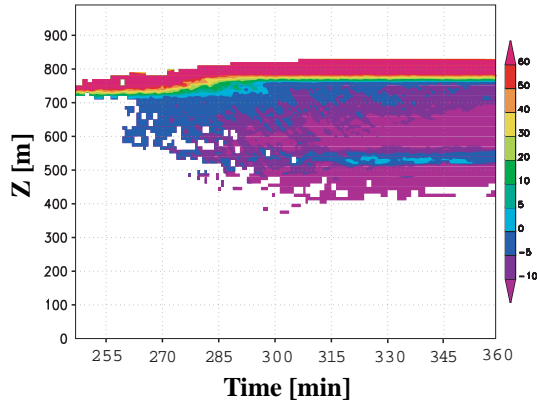


Figure 7. Supersaturation forcing (τ_r) for 200 μm cloud drops as a function of time and with LW cooling included in drop growth.

small drops ($r \sim 5 \mu\text{m}$) and larger drops ($r \sim 200 \mu\text{m}$) are strongly affected by LW radiative cooling throughout the cloud. Small drops are primarily affected by the LW radiative term at cloud top. Since small drops evaporate at the expense of large drops all along cloud top, evaporation occurs along cloud top (not shown). Below cloud top, there is very little influence of radiation on small drop growth and the growth field (not shown) is visually similar to that of the no radiation case (Fig. 6).

The case of large drops is, however, quite different. As was shown for the single parcel, large drops at cloud top experience ever increasing vapor growth because the radiative cooling term increases with size (Fig. 7). However, note that the growth rate throughout the lower part of the cloud is also strongly affected. This is especially true near cloud base ($\sim 500 \text{ m}$) where cloud base LW warming causes strong evaporation of larger drops.

When SW absorption is also included in the vapor growth equation, the growth of both small and large drops are impacted throughout the cloud (Fig. 8) In the case of small drops, evaporation at cloud top still occurs, has the same structure as that of LW cooling, but is reduced in magnitude (not shown). Larger drops ($r \sim 200 \mu\text{m}$), however, are strongly impacted by SW heating throughout the cloud (Fig. 8). Similarly to Fig. 5 for the cloud-top parcel, evaporation of larger drops occurs in every parcel that tracks along cloud top (Fig. 8). Below cloud top, where the maximum in net radiative heating occurs, large drop evaporation rates reach their maximum. Since SW heating is felt throughout most of the cloud layer,

large drops tend to evaporate over much of the depth of the cloud. The only location where growth appears to occur is just

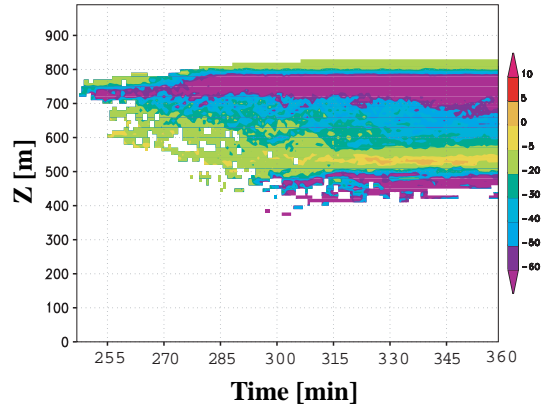


Figure 8. Supersaturation forcing (τ_r) for a 200 μm cloud drops as a function of time and with LW cooling and SW heating included in drop growth.

above cloud base, but below the LW heating maximum. We expect that these size-dependent impacts of SW heating on drop growth have important impacts on the drop size distribution throughout the cloud. We plan to explore this issue in the future.

4.2 Influences on Collision-Coalescence

It is difficult to assess the indirect cloud-scale influence of LW cooling and SW heating on the collision-coalescence process. In order to come to some sort of understanding of how great an influence both SW and LW heating/cooling may be having, we characterized drizzle onset using the predominant radius (cube-root of the ratio of the second moment of the mass distribution to the first), r_p . Austin et al. (1995) imply that $r_{p,\text{lim}} = 45 \mu\text{m}$ is a good indicator for drizzle initiation in stratocumulus. Hence, we computed the amount of time for drops in each parcel to reach $r_{p,\text{lim}}$ (τ_{rp}), which we take to be a measure of the amount of time needed to initiate collision-coalescence. (Studies of ours with the parcel model indicate that this time-scale is a good measure of drizzle initiation for modeled collection.) We then plotted this time-scale against the average amount of time each parcel spent at cloud top. This cloud top residence time is defined as the region over which radiative cooling takes place. Finally, we differenced the time-scales for drizzle production (τ_{rp}) between the no radiation, LW cooling, and LW+SW cooling/heating cases the results of which are shown in Fig. 9a and b. This gives a measure of the reduction in drizzle onset time for each parcel (provided that parcel produces drizzle, otherwise the result is set to zero).

For the case of LW cooling only, one can see that there is a significant reduction in the amount of time required for driz-

zle production. (This turns out to be true regardless of the value of $r_{p,lim}$ that we use, provided the value is greater than about 20 μm .) As one might expect, the largest drizzle onset time-reduction occurs for parcels in the 10 - 30 min cloud top residence time regime. These are the parcels that do not spend a great enough time in the vicinity of the high cloud-top LWC to initiate collision-coalescence. Consequently, these trajectories are the most heavily impacted by the inclusion of LW cooling. In these shorter cloud top residence time cases, drizzle production occurs as much as 35 min earlier. As cloud top residence time becomes longer, most parcels appear to have a reduction in their time for drizzle onset of roughly 10 - 15 minutes.

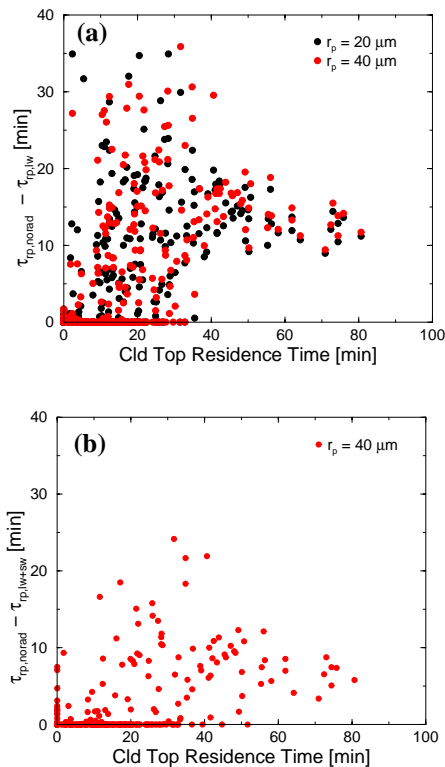


Figure 9. Difference in τ_{tp} with (a) LW cooling and (b) LW cooling + SW heating as a function of cloud top residence time.

When SW heating is included with LW cooling, the impacts on collision-coalescence are less dramatic (Fig. 9b). There is no longer as great of a dependence of the τ_{tp} difference on cloud top residence time. Furthermore, reductions in the time-scale for drizzle onset is about 10 minutes for almost all parcels. Note also that, in comparison to Fig. 9a, there is a lower density in the total number of points plotted. This is a result of the fact that some parcels, under the influence of SW heating, no longer produce drizzle.

The above indirect influence of SW heating on collision-coalescence appears to depend on two things. First, SW heating reduces the total cooling that drops experience. Therefore, the overall growth rate of drops at cloud top will be reduced. Second, large drops experience strong subsaturations (as large as 3-5%, see Harrington and Hartman, 2002). This produces a narrowing of the drop distribution at larger sizes (Fig. 3) which likely also reduces collision-coalescence.

ACKNOWLEDGEMENTS

Chris Hartman's summer REU support, and support for Hans Verlinde, was through NSF grant #9873643.

REFERENCES

- Ackerman, A.S., O.B. Toon, and P.V. Hobbs, 1995: A model for particle microphysics, turbulent mixing, and radiative transfer in the stratocumulus-topped marine boundary layer and comparisons with measurements. *J. Atmos. Sci.*, **52**, 1204-1236.
- Austin, P.H., S. Siems, and Y. Wang, 1995: Constraints on droplet growth in radiatively cooled stratocumulus. *J. Geophys. Res.*, **100**, 14231-14242.
- Barkstrom, B.R., 1978: Some effects of 8-12 micron radiant energy transfer on the mass and heat budgets of cloud droplets. *J. Atmos. Sci.*, **35**, 665-667.
- Bott, A., U. Sievers, and W. Zundkowski, 1990: A radiation fog model with a detailed treatment of the interaction between radiative transfer and fog microphysics. *J. Atmos. Sci.*, **47**, 2153-2166.
- Feingold, G., S.M. Kreidenweis, B. Stevens, and W.R. Cotton, 1996: Numerical simulations of stratocumulus processing of cloud condensation nuclei through collision-coalescence. *J. Geophys. Res.*, **101**, 21 391 - 21 402.
- Fuchs, N.A., 1959: *Evaporation and Droplet Growth in Gaseous Media*. Pergamon Press, 72pp.
- Guzzi, R. and R. Rizzi, 1980: The effect of radiative exchange on the growth of a populations of droplets. *Contrib. Atmos. Phys.*, **53**, 351-365.
- Harrington J.Y., G. Feingold, and W.R. Cotton, 2000: Radiative impacts on the growth of a population of drops within simulated summertime arctic stratus. *J. Atmos. Sci.*, **57**, 766-785.
- Harrington, J. Y., and P. Q. Olsson, 2001: A method for the parameterization of optical properties in bulk and bin microphysical models. Implications for Arctic cloudy boundary layers. *Atmos. Res.*, **57**, 51-80.
- Harrington, J.Y., and C. Hartman, 2002: Drop equilibrium in the presence of solar absorption. In proceedings *11th Conference on Cloud Physics*, 3-7 June, Ogden, Utah, American Meteorological Society.

- Roach, 1976: On the effect of radiative exchange on the growth by condensation of a cloud or fog droplet. *Quart. J. Roy. Meteorol. Soc.*, **102**, 361-372.
- Stevens, B.B., G. Feingold, W.R. Cotton, and R.L. Walko, 1996: Elements of the microphysical structure of numerically simulated nonprecipitating stratocumulus. *J. Atmos. Sci.*, **53**, 980-1006.
- Wiscombe, W. J., R. M. Welch, and W. D. Hall, 1984: The effects of very large drops on cloud absorption. Part I: Parcel Models. *J. Atmos. Sci.*, **41**, 1336-1355.